ISSN 1995-0780, Nanotechnologies in Russia, 2012, Vol. 7, Nos. 1–2, pp. 6–14. © Pleiades Publishing, Ltd., 2012.
Original Russian Text © V.A. Sazhnikov, A.M. Muzafarov, V.N. Kopysov, V.M. Aristarkhov, Yu.N. Kononevich, I.B. Meshkov, N.V. Voronina, M.V. Alfimov , 2012, published in Rossiiskie Nanotekhnologii, 2012, Vol. 7, Nos. 1–2.

Silica Nanoparticles with Covalently Attached Fluorophore as Selective Analyte-Responsive Supramolecular Chemoreceptors

V. A. Sazhnikov[a], **A. M. Muzafarov**[b], **V. N. Kopysov**[a, c], **V. M. Aristarkhov**[a], **Yu. N. Kononevich**[b], **I. B. Meshkov**[b], **N. V. Voronina**[b], **and M. V. Alfimov**[a]

[a] *Photochemistry Center, Russian Academy of Sciences, ul. Novatorov 7A, k. 1, Moscow, 1119421*
[b] *Enikolopov Institute of Synthetic Polymer Materials, Russian Academy of Sciences, ul. Profsoyuznaya 70, Moscow, 117393*
[c] *Moscow Institute of Physics and Technology (State University), Institutskii per. 9, Dolgoprudnyi, Moscow oblast, 141700*
e-mail: sazhnikov@yandex.ru

Received October 10, 2011; accepted for publication October 19, 2011

Abstract—Silica core-shell nanoparticles with SiO_2 cores and an alkoxysilyl derivative of dibenzoylmethanatoboron difluoride (A-$DBMBF_2$) fluorophore covalently attached to the core surface have been synthesized. It is shown that these nanoparticles can be used as the basis of selective sensor materials capable of detecting benzene, toluene, and xylene vapors. As benzene or its methyl derivatives are adsorbed on the surface of nanoparticles, a quenching of A-$DBMBF_2$ fluorescence occurs while an A-$DBMBF_2$/analyte exciplex fluorescence buildup emerges. The position of isoemissive points in the fluorescence spectra is specific for each analyte and can be used for its identification.

DOI: 10.1134/S1995078012010144

INTRODUCTION

The problem of detecting benzene, toluene, and xylene (BTX) vapors is very topical because these compounds are widely used in industry and are present in automobile exhaust. Since compounds of the BTX group are carcinogenic-active substances, they are dangerous even at very low concentrations in the air (at the ppm-ppb level). Therefore, both a search for new sensor materials of high sensitivity to BTX and the development of various portable sensor devices capable of detecting BTX are currently in progress [1–5].

It has been shown recently that dibenzoylmethanatoboron difluoride ($DBMBF_2$) adsorbed on silica microparticles forms exciplexes with methyl derivatives of benzene when they are sorbed from gaseous phase [6, 7]. When toluene or xylene vapors appear in the air, quenching of the fluorescence of adsorbed $DBMBF_2$ and buildup of the fluorescence of the corresponding exciplexes take place simultaneously. If a sample is exposed to ethanol or acetone vapors, only fluorescence quenching is observed. It is clear that this observation makes it possible to develop selective optical materials based on $DBMBF_2$.

The sensitivity of a fluorescent sensor material and its response time are first and foremost determined by the number of fluorophore indicators and their availability for interaction with the molecules of analytes. The use of nanoparticles with indicator molecules immobilized within the surface layer makes it possible to meet both these conditions [8, 9]. It is also noteworthy that, if core-shell nanoparticles are used, it becomes possible to form more complex cores, including either metal cores to use the plasmon resonance effect [10] or an additional fluorophore to use its fluorescence as a reference signal [11, 12].

This work is aimed at synthesizing silica nanoparticles with a core of SiO_2 and a shell of covalently grafted $DBMBF_2$, as well as studying the responses of sensor layers obtained by depositing synthesized nanoparticles onto thin-layer chromotography (TLC) plates to the presence of BTX vapors.

EXPERIMENTAL

Synthesis Of $DBMBF_2$ and Nanoparticles

Investigation Techniques

The spectra of NMR ^1H, ^{13}C, ^{19}F were measured on a BrukerAvanceII 300 spectrometer. The IR spectra were registered on a Bruker Equinox 55/S device. Electronic microphotographs were obtained using a (TEM) LEO 912 ABOMEGA (Germany) transmission electron microscope.

Synthesis of Silica on the Basis of Tetraethoxysilane (TEOS) Using the Stöber Technique

Twenty-two milliliters of ethanol and 0.9 ml of 23% aqual ammonia were placed into a flat-bottomed bulb with stirring and 1.6 ml of TEOS was added. The stirring continued for 24 h. When the reaction ended, the reaction mixture was spun for 15 min. The upper layer of the reaction mixture was poured out and tetrahydrofuran (THF) was added to the precipitate. The resulting product was dispersed using an ultrasound bath for 10 min at a temperature of 25°C. Then the spinning was repeated once more, the upper layer was poured out and sent to utilization, and a fresh tetrahydrofuran was added to the precipitate and dispersed in an ultrasound bath. The operations of spinning and dispersion were repeated two more times.

Synthesis of 1-PHENYL-3-[4-METHYLPHENYL]PROPANE-1,3-DIONE ***2***

The solution of 4-methylacetophenone (0.05 mol) and ethyl benzoate (0.05 mol) in tetrahydrofuran (20 ml) was added to the suspension of sodium hydride (0.055 mol) in tetrahydrofuran (20 ml). The resulting mixture was stirred as it boiled for 8 h. The reaction mixture was cooled down to room temperature and poured out into an aqueous solution of acetic acid (5%, 100 ml). The precipitate was filtered and recrystallized from isopropyl alcohol. The yield was 81%. T_{melt} = 81–82°C. UV (CsI): 3467, 3039, 1604, 1543, 1485, 1309, 1232, 1188, 1020, 771 cm^{-1}. ^{1}H NMR (300 MHz, DMSO-d$_6$): δ 2.43 s, 3H, CH$_3$), 6.84 (s, 1H, CO-CH-CO), 7.24–7.30 (m, 2H, Ar), 7.45–7.58 (m, 3H, Ar), 7.88–7.99 (m, 4H, Ar), 11.39 (s, 1H, OH). ^{13}C NMR (75 MHz, CDCl$_3$): δ 21.6, 92.8, 127.1, 127.2, 128.6, 129.4, 132.2, 133.0, 135.7, 143.2, 185.2, 186.0. UV (THF) λ = 348 nm (ε = 29500 l/mol · cm). HRMS (ESI) *m/z* calculated for $C_{16}H_{14}NaO_2$ [(M + Na)$^+$]: 261.0886, found 261.0885. The elemental analysis, calculated (%) for $C_{16}H_{14}O_2$: C, 80.65; H, 5.92. Found: C, 80.86; H, 6.01.

Synthesis of 2,2-DIFLUORO-4-PHENYL-6-[4-METHYLPHENYL]-1,3,2-(2H)-DIOXABORINE ***3***

Boron trifluoride ether (0.012 mol) was added with stirring to the solution of β-diketone **2** (0.01 mol) in dichloromethane (30 ml). The reaction mixture was stirred at room temperature for 1 h. After the solvent had been removed in vacuum, the precipitate was recrystallized from toluene. The yield was 87%. T_{melt} = 205–206°C. IR (CsI): 3167, 1603, 1543, 1493, 1371, 1315, 1252, 1043 cm^{-1}. ^{1}H NMR (300 MHz, DMSO-d$_6$): δ 2.47 (c, 3H, CH3), 7.51 (d, 2H, J = 8.5 Hz, Ar), 7.68 (t, 2H, J$_1$ = 7.3 Hz, J$_2$ = 7.9 Hz, Ar), 7.83 (t, 1H, J = 7.3 Hz, Ar), 7.93 (c, 1H, CO–CH–CO), 8.32 (d, 2H, J = 7.9 Hz, Ar), 8.39 (d, 2H, J = 7.3 Hz, Ar). ^{1}H NMR (300 MHz, DMSO-d$_6$): δ 2.47 (s, 3H, CH$_3$), 7.51 (d, 2H, J = 8.5 Hz, Ar), 7.68 (t, 2H, J$_1$ = 7.3 Hz, J$_2$ = 7.9 Hz, Ar), 7.83 (t, 1H, J = 7.3 Hz, Ar), 7.93 (s, 1H, CO-CH-CO), 8.32 (d, 2H, J = 7.9 Hz, Ar), 8.39 (d, 2H, J = 7.3 Hz, Ar). ^{13}C NMR (75 MHz, CDCl$_3$): δ 21.9, 93.1, 128.8, 129.1, 129.3, 130.0, 132.2, 135.0, 147., 182.6, 183.3. ^{19}F NMR (282 MHz, CDCl$_3$): δ – 141.05 (21%, ^{10}B–F), – 141.12 (79%, ^{11}B–F). UV (THF) λ = 370 nm (ε = 43900 l/mol · cm). HRMS (ESI) *m/z* calculated for $C_{16}H_{13}BF_2NaO_2$ [(M + Na)$^+$]: 309.0872, found 309.0872. The elemental analysis, calculated (%) for $C_{16}H_{13}BF_2O_2$: C, 67.17; H, 4.58; B, 3.78; F, 13.28. Found: C, 58.86; H, 4.56; B, 4.24; F, 15.26.

Synthesis of 2,2-DIFLUORO-4-PHENYL-6-[4-BROMOMETHYLPHENYL]-1,3,2-(2H)-DIOXABORINE ***4***

The mixture of boron difluoride β-diketonate**3** (0.01 mol), N-bromosuccinimide (0.01 mol), and azobisisobutyronitrile (50 mg) was boiled in carbon tetrachloride for 4 h. After having removed the solvent in vacuum, the precipitate was purified by chromotography in a column with silica gel (an eluent was toluene, R_f = 0.43). The yield was 67%. T_{melt} = 178–180°C. IR (CsI): 1549, 1491, 1375, 1041, 717 cm^{-1}. ^{1}H NMR (300 MHz, CDCl$_3$): δ 4.52 (s, 2H, CH$_2$Br), 7.18 (s, 1H, CO–CH–CO), 7.56 (m, 4H, Ar), 7.71 (t, 1H, J = 7.3 Hz, Ar), 8.14 (m, 4H, Ar). ^{13}C NMR (75 MHz, DMSO-d$_6$): δ 32.8, 94.8, 129.4, 129.5, 129.8, 130.2, 131.0, 131.3, 136.0, 146.1, 181.9, 182.8. ^{19}F NMR (282 MHz, CDCl$_3$): δ –140.53 (21%, ^{10}B–F), –140.59 (79%, ^{11}B–F). UV (THF) λ = 370 nm (ε = 48600 l/mol · cm). HRMS (ESI) *m/z* calculated for $C_{16}H_{12}BF_2BrNaO_2$ [(M + Na)$^+$]: 386.9977, found 386.9974. The elemental analysis, calculated (%) for $C_{16}H_{12}BF_2BrO_2$: C, 52.65; H, 3.31; B, 2.96; F, 10.41; Br, 21.89. Found: C, 52.41; H, 3.13; B, 2.96; F, 10.32; Br, 21.68.

Synthesis of Alkoxysilyl Derivative of Dibenzoylmethanatoboron Difluoride ***5*** *(A-DBMBF$_2$)*

A mixture of a brom derivative of boron difluoride β-diketonate **4** (0.003 mol), 3-mercaptopropylmethyldimethoxisilane (0.003 mol), and triethylamine (0.003 mol) was stirred at room temperature for 2 h. The resulting product was used to immobilize nanoparticles.

Modification of the Surface of Silica Nanoparticles with Alkoxysilyl Derivative of Dibenzoylmethanatoboron Difluoride

An alkoxysilyl derivative of dibenzoylmethanatoboron fluoride **5** was dissolved in THF (5 ml), and nanoparticles (0.4 g) obtained by the Stöber method and dispersed in THF were added to the solution. A bulb with the resulting reaction mass was placed into an ultrasound bath and heated up to 50°C for 5 h. After the reaction ended, the reaction mixture was spun for 5 min at a spin-rotor rotation speed of 6000 rpm. The upper layer of the reaction mixture was poured out, and fresh THF was added to the precipitate.

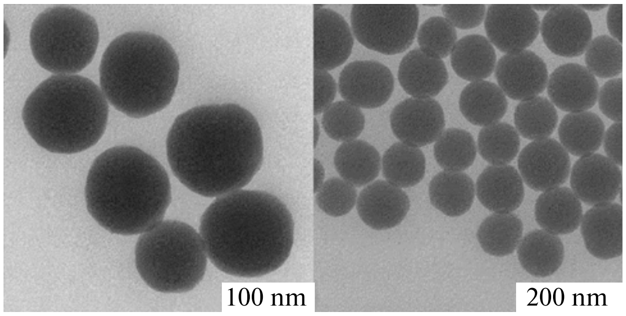

Fig. 1. Microphotographs of SiO_2 particles obtained by the Stöber method.

The resulting product was dispersed in an ultrasound bath for 10 min at a temperature of 25°C. Then the spinning was repeated once more, the upper layer was poured out and sent to utilization, and fresh THF was added to the precipitate and dispersed in an ultrasound bath. The operations of spinning and dispersion were repeated two more times.

Registration of Responses of Sensor Layers Based on Nanoparticles

Benzene, toluene, and xylenes (Aldrich, spectroscopic grade) were used as received.

Thin-layer chromatography plates (TLC plates) by Sorbfil (the working layer of the sorbent was silica gel of the brand STC-1A, 90–120 μm thick, fixed with a binder based on silica sol) were used as matrices for the immobilization of nanoparticles. The sorbent particles were 5–17 μm in size.

Squares of about 25 × 25 mm were cut out of the TLC plates, and one or several drops (0.05 ml) of dispersion of nanoparticles in THF were deposited onto their surface; then they stored for 1 h until the complete evaporation of the solvent. The fluorescence emission and fluorescence excitation spectra were registered using a Shimadzu RF5301-PC spectrofluorimeter.

To study the responses of samples to the presence of analyte vapors, the samples were placed on a stand in a closed box with a volume of 1.7 l, where a definite pressure of BTX vapors were created by evaporating a certain amount of solvent (as a rule, 0.05–0.15 ml). To achieve a homogeneous distribution of the vapors within the volume, a small electrical fan was placed inside the box. Changes in the fluorescence spectra were registered using an R400-7 UV/VIS fiber-optic fluorescent probe inserted into the box and attached to a D-2000 Ocean Optics fiber-optic spectrofluorimeter. As a light source, a light-emitting diode with a wavelength of 375 nm was used. The fluorescence responses of the layers at low concentrations of analytes (10–50 ppm) were obtained using an experimental system for investigating the characteristics of optical sensor materials [13].

RESULTS AND DISCUSSION

Synthesis of Nanoparticles and Their Properties

Technical difficulties in the application of a relatively low-molecular and nonfunctional dye have promoted the development of its functionalization technique and attachment to the surface of silica particles. The general scheme of the synthesis consists of three basic stages: the synthesis of a nanodimensional silica gel, the synthesis of a functionalized dye, and the attachment of the dye to the surface of silica particles. At the first stage, monodispersive silica nanoparticles were obtained using the method of hydrolytic polycondensation of tetraethoxisilane in a mixture of ethanol, water, and ammonia according to the known technique [14] (Fig. 1).

In this case, we can observe isolated spherical particles with the dimensions amounting to 90–100 nm.

The synthesis of an alkoxysilyl derivative of dibenzoylmethanatoboron difluoride (A-DBMBF$_2$) was achieved in several stages (Scheme 1) from β-diketone **2**, which was obtained by the Claisen condensation between 4-methylacetophenone and ethyl benzoate in the presence of sodium hydride in tetrahydrofuran. The complex of boron difluoride **3** was obtained by the reaction of β-diketone **2** with boron trifluoride ether in dichloromethane. After the reaction was completed, the solvent was removed in vacuum and the rest was recrystallized from toluene. Bromoderivative **4** was obtained from β-diketonate of boron difluoride **3** by a free-radical bromination of the latter with N-bromosuccinimide in carbon tetrachloride. A nucleophylic substitution of bromine atom in the compound **4** 3-mercaptopropylmethyldimethoxisilane in the presence of triethylamine made it possible to obtain an alkoxysilyl derivative of dibenzoylmethanatoboron difluoride.

The subsequent attachment of A-DBMBF$_2$ to the surface of SiO_2 nanoparticles was achieved using the reaction of condensation of compound **5** with silica particles obtained by the Stöber technique according to the reaction shown in Scheme 2.

After the synthesis was finished, the particles were rinsed in an organic solvent to clean them from nonreacted residues and other low-molecular impurities.

Microphotographs of nanoparticles with dibenzoylmethanatoboron difluoride attached to them are shown in Fig. 2.

Changes in the Fluorescence of Modified Nanoparticles in the Presence of Vapors of Aromatic Molecules

Figure 3 shows the fluorescence excitation and emission spectra of nanoparticles with the grafted A-DBMBF$_2$ dispersed within the functional layer of a TLC plate. In general, these spectra are very close

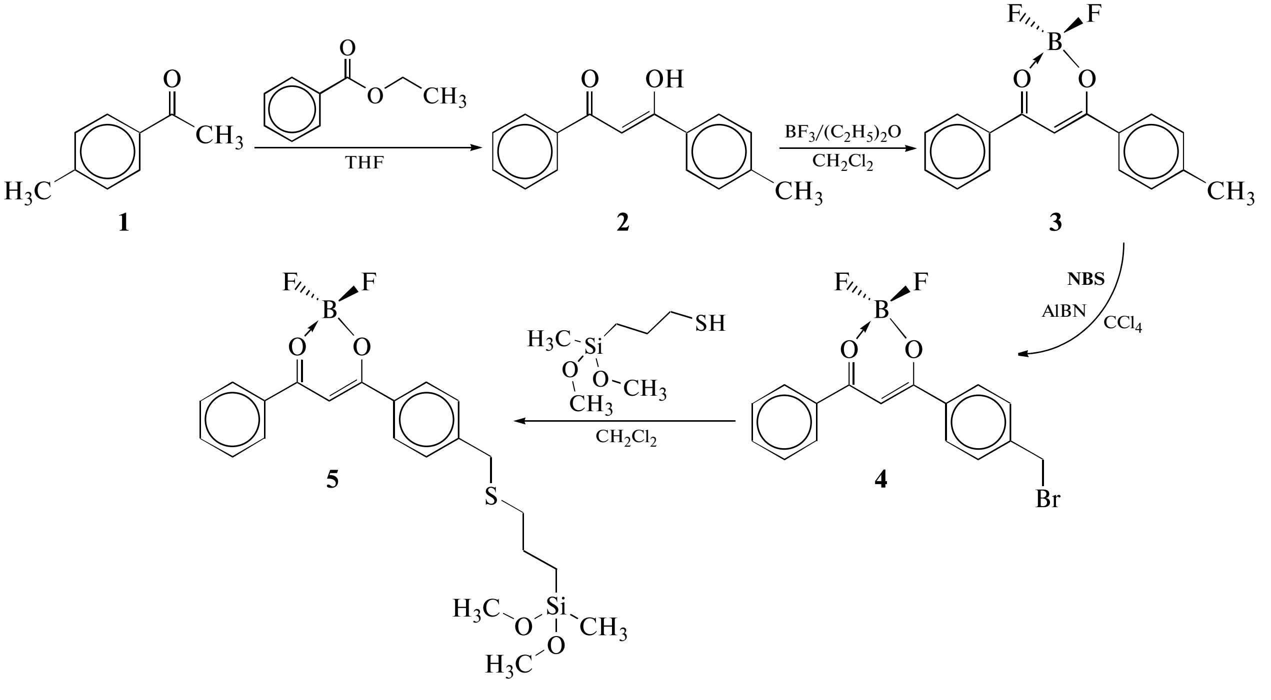

Scheme 1. Scheme of the synthesis of alkoxysilyl derivative of dibenzoylmethanatoboron difluoride.

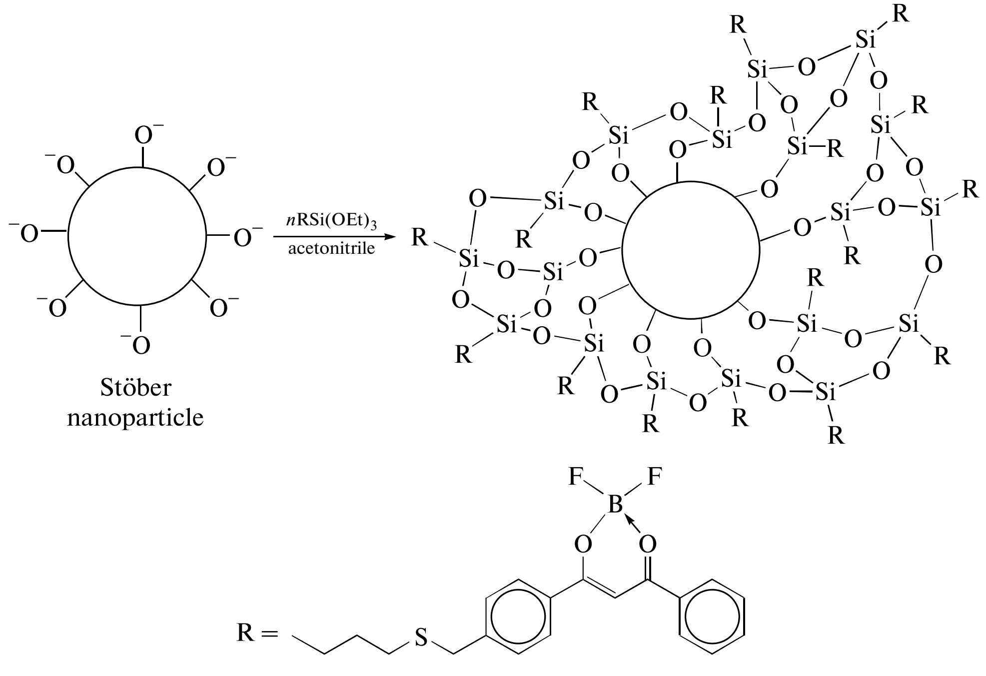

Scheme 2. Scheme of the synthesis of nanoparticles with an attached dibenzoylmethanatoboron difluoride.

to those of the parent $DBMBF_2$ adsorbed on a TLC plate [6].

It should be noted that the position of the maximum of the A-$DBMBF_2$ fluorescence band depends on the contribution of excimers and dimers into the fluorescence emission spectrum, as well as on the spectral width of the exciting light. The broad fluorescence spectrum of excimers and dimers has a maximum in the region of 500 nm [7]. The fluorescence excitation spectrum of excimers coincides with that of the monomers. An additional band in the region of 420–430 nm is also present in the fluorescence excita-

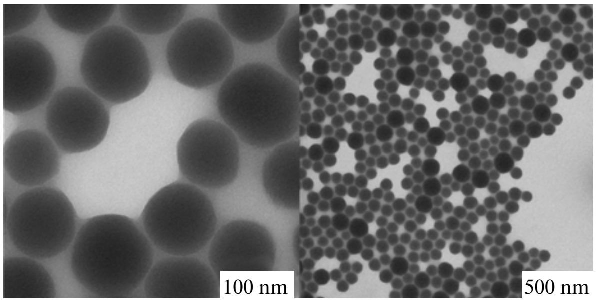

Fig. 2. TEM microphotographs of SiO_2 particles with an attached derivative of dibenzoylmethanatoboron difluoride.

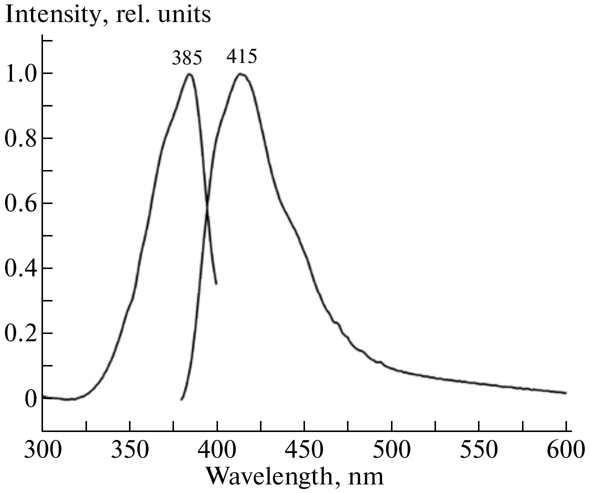

Fig. 3. The fluorescence emission (on the right, λ_{exc} = 365 nm) and fluorescence excitation spectra (on the left, λ_{observ} = 413 nm).

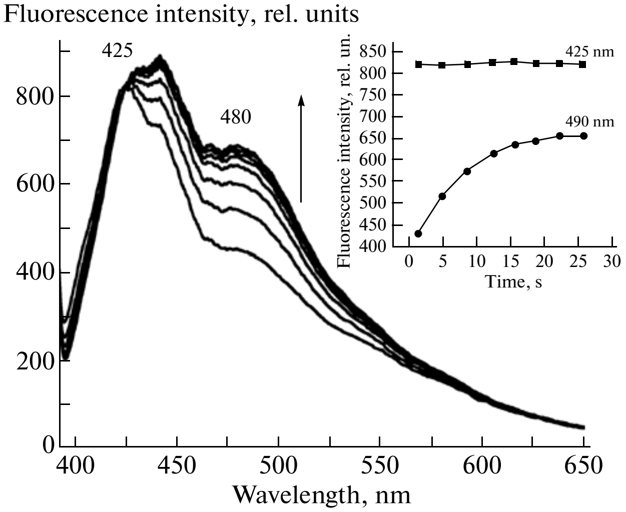

Fig. 4. A change in the fluorescence spectrum of the sample (λ_{exc} = 375 nm) with time upon exposure to benzene vapors (C = 30000 ppm). The spectra were registered with an interval of 4 s. The insert shows the kinetics of fluorescence intensity changes at two wavelengths (425 and 490 nm).

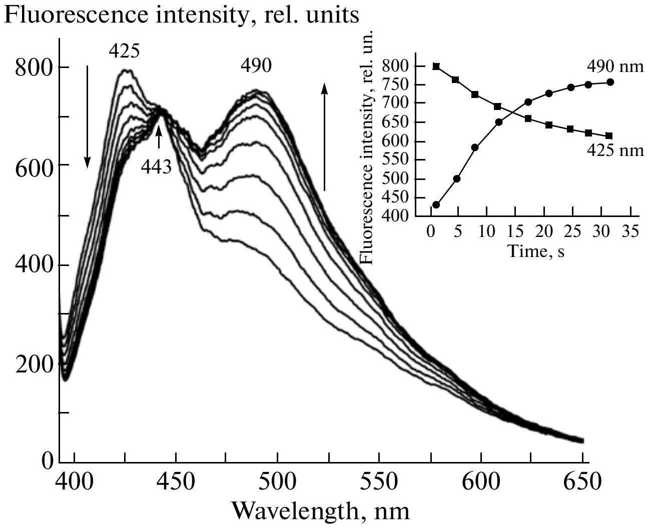

Fig. 5. A change in the sample fluorescence spectrum (λ_{exc} = 375 nm) with time upon exposure to toluene vapors (C = 20000 ppm). The spectra were registered with an interval of 4 s. The insert shows the kinetics of the fluorescence intensity changes at two wavelengths (425 and 490 nm).

tion spectrum for samples with a high A-$DBMBF_2$ concentration, which corresponds to the absorption of dimers. The spectra shown in Fig. 3 correspond to a sample in which the contribution of excimer and dimer fluorescence is minimal.

Studies of the responses to the vapors of analytes were carried out on the samples where the contribution of excimers and dimers is high enough and the fluorescence band maximum is shifted towards the long-wavelength region and is localized in the region of 420–425 nm.

Figures 4–8 show time-dependent changes in the fluorescence spectra of samples upon exposure to vapors of benzene, toluene, and ortho-, meta-, and para-xylene, respectively. The fluorescence spectra were obtained at every 4 s from the beginning of exposure. It can be seen that, along with the fluorescence quenching in the region of 400–425 nm corresponding to the A-$DBMBF_2$ monomer fluorescence, an intensity increase in the region of 430–520 nm is also observed. In the case of benzene vapors, the A-$DBMBF_2$ fluorescence quenching is not observable

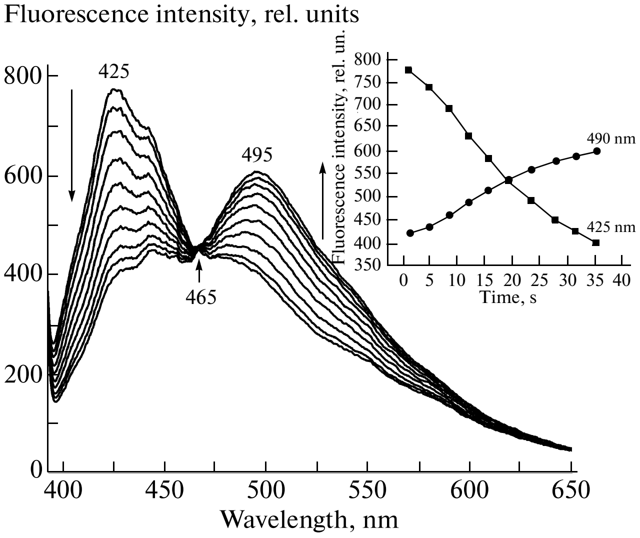

Fig. 6. A change in the fluorescence spectrum of the sample (λ_{exc} = 375 nm) with time upon exposure to meta-xylene vapors (C = 6000 ppm). The spectra were registered with an interval of 4 s. The insert shows the kinetics of the fluorescence intensity change at two wavelengths (425 and 490 nm).

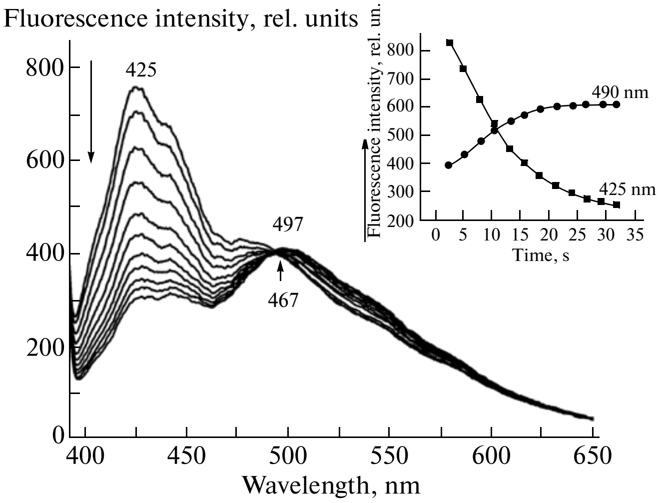

Fig. 7. A change in the fluorescence spectrum of the sample (λ_{exc} = 375 nm) with time upon exposure to ortho-xylene vapors (C = 6000 ppm). The spectra were registered with an interval of 4 s. The insert shows the kinetics of the fluorescence intensity change at two wavelengths (425 and 490 nm).

against the background of long-wavelength band growth.

It is noteworthy that the character of spectral changes for a covalently grafted A-$DBMBF_2$ in the case of toluene and m-xylene is similar to the spectral changes observed for $DBMBF_2$, adsorbed on a TLC layer [6, 7]. It follows from a comparison of our data and those of [6, 7], as well as the literature data that the emission in the longer wavelengths region should be attributed to the fluorescence of exciplexes A-$DBMBF_2$/analyte, which are formed as a result of the interaction between the molecule of analyte and the electronically-excited molecule of the fluorophore.

The most interesting and important from the point of view of response peculiarities depending on the analyte structure is the existence of characteristic isoemissive points for each analyte. It can be seen from our figures that the isoemissive points are located at 425, 440, 465, and 495 nm for benzene, toluene, m-xylene, and p-xylene, respectively. It is seen that the isoemissive point for benzene is located in the neighborhood of the monomer fluorescence maximum (425 nm), while for toluene it shifts to 440 nm. Spectral changes for o-xylene are practically identical with those for m-xylene; the locations of the isoemissive points coincide as well (465 nm). However, a further rather great (by about 30 nm) bathochromic shift of the isoemissive point is observed for p-xylene.

Thus, the position of isoemissive points differs markedly in the benzene-toluene-xylenes family, so it can be used for an decisive identification of the analytes. For example, it is seen from the kinetic curves of changes in the fluorescence intensity at wavelengths of 425 and 490 nm shown in the inserts to Figs. 4–8 that the fluorescence intensity at 425 nm in the case of benzene and at 490 nm in the case of p-xylene is not changed.

It is clear from the data that, if the analytes are present in high concentrations, they can be detected either by a decrease in the monomer fluorescence intensity or by an increase in the fluorescence intensity of the corresponding exciplex. The choice of the mode

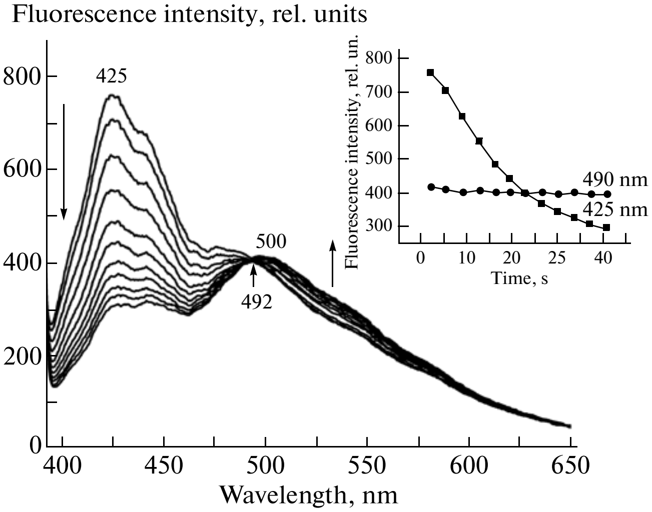

Fig. 8. A change in the fluorescence spectrum of the sample (λ_{exc} = 375 nm) with time upon exposure to para-xylene vapors (C = 5000 million^{-1}). The spectra were registered with an interval of 4 s. The insert shows the kinetics of the fluorescence intensity change at two wavelengths (425 and 490 nm).

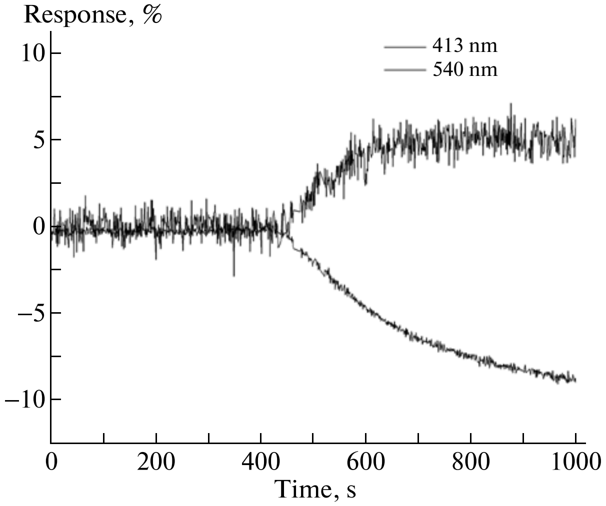

Fig. 9. The response of the sample to being exposed to ortho-xylene vapors (C = 12 million^{-1}). The arrow shows the moment of o-xylene admission.

is determined by the convenience of observation at one or another wavelength. The response time depends on a number of factors, in particular, on the diffusion rate of analyte molecules into the layer, as well as inside it. For the samples studied, this amounts to about several tens of seconds (see inserts to Figs. 4–8). By changing the composition and structure of the sensor layer, we can vary the response time within wide limits.

The character of the observed spectral changes is illustrated in these figures for the analyte concentrations close to those for their saturated vapors. To test the possibility of measuring low concentrations of BTX with the help of the layers, we studied the responses to one of the analytes having a concentration close to its PEL value. Figure 9 shows the sample fluorescent response to the presence of 12 ppm o-xylene. It is seen that the changes in the fluorescence intensity at two wavelengths corresponding to monomer (413 nm) and exciplex (540 nm) are sufficient for a reliable registration of the appearance of o-xylene vapors even at such a low concentration. The response time in this case, however, is much greater.

Let us qualitatively describe in brief the mechanism of the phenomena observed. A schematic representation of the shell structure of synthesized silica nanoparticles is shown in Fig. 10. The estimated mean surface density of covalently attached fluorophore molecules amounts to about 0.75 mol/nm^2. The similarity between excitation and emission spectra for the adsorbed $DBMBF_2$ and covalently grafted A-$DBMBF_2$ proves that the microenvironment in both cases is similar. Since the adsorbtion of $DBMBF_2$ is likely achieved mainly at the expense of hydrogen bonds, we can conclude that the covalently immobilized molecules of A-$DBMBF_2$ also interact mainly with the surface silanol groups. In this case, some of them probably remain in a free state and the molecules located close to each other form complexes of various types. According to the literature data, a typical density of silanol groups is about 3–5 OH/nm^2 [15]. Thus, we should suggest that several silanol groups are located near each fluorophore molecule and they form its polar microenvironment. Quantum-chemical calculations of a simplest model of the interaction between a molecule of $DBMBF_2$ and one silanol group lead to the conclusion that the energy of such an interaction is equal to about 10 kcal/mol [7]. This means that the major part of the immobilized A-$DBMBF_2$ molecules in the ground state form a complex at least with one of OH groups located at the corresponding distance from the bonding center. Thus, we can assume that these supramolecular A-$DBMBF_2$/OH complexes (with an A-$DBMBF_2$ molecule temporarily fixed in a definite position) are just the main receptor centers which bind analyte molecules.

The presence of the excimer emission in the fluorescence spectra in the wavelength region of 480–520 nm indicates that some of the attached molecules are located close enough to each other (see Fig. 10) and form either dimers in the ground state or exciplexes in excited states.

According to available literature data, molecules of benzene, toluene, and xylene in the gas phase can be sorbed to the surface of silicate particles and rather easily (especially while at low concentrations) diffuse along the surface of particles. Hydrogen bonds between π electrons of aromatic molecules and silanol OH groups are of first importance in the sorption and diffusion processes [16–19].

It is evident that if different molecules with corresponding donor and acceptor properties are adsorbed at the surface, then the formation of donor–acceptor complexes is possible due to their diffusion. In particular, the exciplex formation process at the surface of SiO_2 was studied in [20] for the case when molecules of pyrene and dimethylaniline were adsorbed at silica gel.

Thus, the process of exciplex formation in the samples under study can be represented as follows. When a molecule of A-$DBMBF_2$ is electronically excited, its interaction with one of the closest sorbed analyte molecules leads to the formation of a fluorescent A-$DBMBF_2$/analyte exciplex. It should be noted that, after exposure the samples to the analyte vapors for some time in the dark, we can observe (by switching on the exciting light) identical intensity exciplex fluorescence as in exposure under the conditions of a continuous illumination with an exciting light. This can mean that a substantial part of fluorophore and analyte molecules already in the ground electron state form weak complexes, which are transformed into exciplexes upon fluorophore excitation.

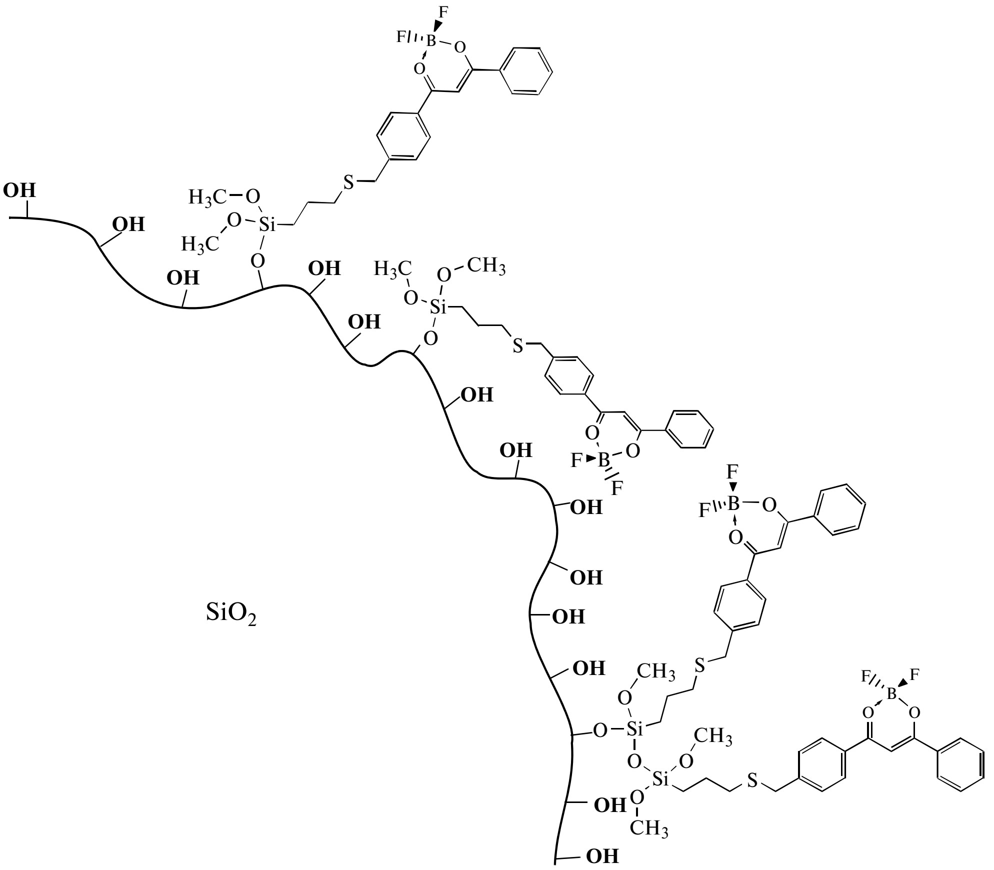

Fig. 10. Schematic representation of the shell structure of synthesized nanoparticles.

It is evident that the position of the exciplex fluorescence maximum and the fluorescence quantum efficiency (and, hence, the position of the isoemissive point) depend on the A-DBMBF$_2$/analyte complex structure. A-DBMBF$_2$ and benzenes are electron-accepting and, respectively, electron-donating subunits of the complexes. The facts that the position of the maximum in the exciplex fluorescence is shifted towards the long-wavelength region concurrently with a reduction in the analyte ionization potential and that similar spectral changes are observed for o- and m-xylenes having the same ionization potentials mean that donor properties of analytes are of first importance in this case.

CONCLUSIONS

Thus, the following main results have been obtained in this work:

An alkoxysilyl derivative of dibenzoylmethanatoboron difluoride fluorophore is synthesized.

The synthesized fluorophor is covalently grafted on the surface of SiO$_2$ nanoparticles.

Based on the synthesized nanoparticles, sensor films are obtained using their dispersion in the layer of silicate microparticles.

The responses of sensor layers to vapors of benzene, toluene, and xylenes are studied, and it is established that, simultaneously with quenching of the fluorophore fluorescence the buildup of the fluorescence of exciplexes fluorophor/analyte takes place.

It is established that the occurrence of isoemissive points is characteristic of the time-dependent fluorescence spectra of studied sensor films. The point position can be used for unique identification of an analyte related to BTX group.

It is shown using the layers based on synthesized nanoparticles, it is possible to register the presence of analytes in the air from the BTX group at concentrations of several tens of ppm.

It should be noted that the structure of synthesized nanoparticles makes it possible to form composite cores with more complex structures, e.g., consisting of metal cores surrounded by the shells of SiO$_2$. The cores of such a composition make it possible to use the phenomenon of plasmon resonance to enhance the output fluorescence signal. Work in this direction is currently in progress.

ACKNOWLEDGMENTS

This work was supported by the Federal Targeted Programme "R&D in Priority Fields of the S&T Complex of Russia (2007-2012)" (State Contract no. 02.527.11.0009, coordinated with the INGENIOUS project of the Seventh European Framework Program, Grant no. 248236).

REFERENCES

1. M.-L. Calvo-Munoz, T.-T. Truong, and T.-H. Tran-Thi, "Chemical Sensors of Monocyclic Aromatic Hydrocarbons Based on Sol–Gel Materials: Kinetics of Trapping of the Pollutants and Sensitivity of the Sensor," Sens. Actuat. B **87** (1), 173–183 (2002).
2. M. Mabrook and P. Hawkins, "Benzene Sensing Using Thin Films of Titanium Dioxide Operating at Room Temperature," Sensors **2** (9), 374–382 (2002).
3. H. Ablat, A. Yimit, M. Mahmut, and K. Itoh, "Nafion Film/K+-Exchanged Glass Optical Waveguide sensor for BTX Detection," Anal. Chem. **80** (20), 7678–7683 (2008).
4. M. A. Rawashdeh-Omary, M. D. Rashdan, S. Dharanipathi, O. Elbjeirami, P. Ramesh, and Y. V. R. Dias, "On/off Luminescence Vapochromic Selective Sensing of Benzene and its Methylated Derivatives by a Trinuclear Silver(I) Pyrazolate Sensor," Chem. Commun. **47** (4), 1160–1162 (2011).
5. E. Sokol, K. E. Edwards, K. Qian, and R. G. Cooks, "Rapid Hydrocarbon Analysis Using a Miniature Rectilinear Ion Trap Mass Spectrometer," Analyst **133** (8), 1064–1071 (2008).
6. V. A. Sazhnikov, V. M. Aristarkhov, A. G. Mirochnik, E. V. Fedorenko, and M. V. Alfimov, "Fluorescence Quenching of Silica Gel–Adsorbed (Dibenzoylmethanato)boron Difluoride by Polar Solvent Vapor," Dokl. Phys. Chem. **437**, 35 (2011).
7. V. A. Sazhnikov, V. M. Aristarkhov, A. A. Safonov, A. A. Bagatur'yants, A. G. Mirochnik, E. V. Fedorenko, and M. V. Alfimov, "Fluorescence Spectra and Structure of the Difluoro(dibenzoylmethanato)boron Monomers and Dimers Absorbed on Silica Gel," Khim. Vysok. Energ. **45** (4), 347 (2011).
8. K. I. Oberg, R. Hodyss, and J. L. Beauchamp, "Simple Optical Sensor for Amine Vapors Based on Dyed Silica Microspheres," Sens. Actuat. B **115** (1), 79–85 (2006).
9. L. Basabe-Desmonts, D. N. Reinhoudt, and M. Crego-Calama, "Design of Fluorescent Materials for Chemical Sensing," Chem. Soc. Rev. **36** (6), 993–1017 (2007).
10. D. Cheng and Q.-H. Xu, "Separation Distance Dependent Fluorescence Enhancement of Fluorescein Isothiocyanate by Silver Nanoparticles," Chem. Commun., No. 3, 248–250 (2007).
11. A. Burns, P. Sengupta, T. Zedayko, B. Baird, and U. Wiesner, "Core/Shell Fluorescent Silica Nanoparticles for Chemical Sensing: Towards Single-Particle Laboratories," Small **2** (6), 723–726 (2006).
12. C. Zong, K. Ai, G. Zhang, H. Li, and L. Lu, "Dual-Emission Fluorescent Silica Nanoparticle-Based Probe for Ultrasensitive Detection of Cu2+," Anal. Chem. **83** (8), 3126–3132 (2011).
13. A. A. Khlebunov, D. S. Ionov, P. V. Komarov, V. M. Aristarkhov, V. A. Sazhnikov, A. N. Petrov, and M. V. Alfimov, "An Experimental System for Investigating the Characteristics of Optical Sensor Materials," Instrum. Exp. Tech. **52**, 132 (2009).
14. W. Stöber, A. Fink, and E. Bohn, "Controlled Growth of Monodisperse Silica Spheres in the Micron Size Range," J. Colloid Interface Sci. **26** (1), 62–69 (1968).
15. A. A. Christy and P. K. Egeberg, "Quantitative Determination of Surface Silanol Groups in Silicagel by Deuterium Exchange Combined with Infrared Spectroscopy and Chemometrics," Analyst **130** (5), 738–744 (2005).
16. S. C. Ringwald and J. E. Pemberton, "Adsorption Interactions of Aromatics and Heteroaromatics with Hydrated and Dehydrated Silica Surfaces by Raman and FTIR Spectroscopies," Environ. Sci. Technol. **34** (2), 259–265 (2000).
17. V. R. Choudhary and K. Mantri, "Adsorption of Aromatic Hydrocarbons on Highly Siliceous MCM-41," Langmuir **16** (17), 7031–7037 (2000).
18. S. J. Reitmeier, R. R. Mukti, A. Jentus, and J. A. Lercher, "Surface Transport Processes and Sticking Probability of Aromatic Molecules in HZSM-5," J. Phys. Chem. C **112** (7), 2538–2544 (2008).
19. A. Rimola, B. Civalleri, and P. Ugliengo, "Physisorption of Aromatic Organic Contaminants at the Surface of Hydrophobic/Hydrophilic Silica Geosorbents: A B3LYP-D Modeling Study," Phys. Chem. Chem. Phys. **12** (24), 6357–6366 (2010).
20. G. Zhang, J. K. Thomas, A. Eremenko, T. Kikteva, and F. Wilkinson, "Photoinduced Charge-Transfer Reaction between Pyrene and N,N'-Dimethylaniline on Silica Gel Surfaces," J. Phys. Chem. **101** (42), 8569–8577 (1997).